Available online at www.sciencedirect.com
SCIENCE DIRECT
Journal of Power Sources 158 (2006) 550–556
JOURNAL OF POWER SOURCES
www.elsevier.com/locate/jpowsour

Kinetic study on low-temperature synthesis of $LiFePO_4$ via solid-state reaction

Hao-Hsun Chang [a], Chun-Chih Chang [a], Hung-Chun Wu [b], Zheng-Zhao Guo [b], Mo-Hua Yang [b], Yung-Ping Chiang [c], Hwo-Shuenn Sheu [c], Nae-Lih Wu [a,*]

[a] *Department of Chemical Engineering, National Taiwan University, Taipei 106, Taiwan, ROC*
[b] *Materials Research Laboratories, Industrial Technology Research Institute, Chutung, Hsinchu 310, Taiwan, ROC*
[c] *National Synchrotron Radiation Research Center, Hsinchu 30077, Taiwan, ROC*

Received 3 July 2005; received in revised form 1 September 2005; accepted 2 September 2005
Available online 2 November 2005

Abstract

Rate equation of $LiFePO_4$ formation via solid-state reaction has been studied by using a model system: $Li(CH_3COO) + FePO_4$ in a reducing atmosphere. Kinetic data were acquired by using in-situ synchrotron X-ray diffraction technique, and the analysis was based on a non-isothermal methodology, which shows that the reaction rate is well described by the rate-equation: $[F^{0.7}/(1-F)^{0.7}] = 1.56 \times 10^{11} \exp(-24{,}100/T)t$, where F is the fractional conversion to $LiFePO_4$, T, the calcination temperature (K), and t is the calcination time (min). The equation indicates that the formation of $LiFePO_4$ is intrinsically a fast reaction: 95% conversion can be achieved between 550 and 600 °C in a few hours. Nevertheless, the reaction could be significantly hindered if gas-phase diffusion processes of reactant/product species become rate-limiting, and the gas-flow pattern relative to the powder bed during synthesis thus has a decisive effect on the reaction rate in large-scale synthesis. Single-phased, nanocrystalline $LiFePO_4$ powder having an average crystal size of 35 nm can be synthesized by calcination using flow-through configuration at 600 °C in merely 2 h, and the powder exhibits a capacity of ~140 mAh g^{-1}.

Keywords: Li-ion battery; Cathode; $LiFePO_4$; Synthesis; Kinetics

1. Introduction

Orthorhombic olivine compound $LiFePO_4$ has drawn considerable attention for its application as a cathode material for lithium ion batteries [1]. This compound has a theoretical capacity of 170 mAh g^{-1}, and is environmentally benign. In addition, compared with other cathode oxide materials, such as $LiCoO_2$ and $LiNiO_2$, $LiFePO_4$ is relatively cheaper and possesses greater thermal stability. Different synthetic routes have so far been reported for synthesizing $LiFePO_4$, and Table 1 summarizes some of the synthesis conditions reported in the literature. It was particularly noticed that fairly wide ranges of thermal conditions, ranging from 550 to 800 °C with a holding time between 0.5 and 24 h, have been employed for obtaining crystalline $LiFePO_4$ [1–12]. Other than Ref. [9], which employed a sol–gel method, the rest have all employed the solid-state reaction approach. No apparent reason for causing these differences in synthesis condition can be elucidated from those reports. Unnecessary prolonged heating not only results in an increase in manufacturing cost but also could deteriorate the performance of the olivine compound. $LiFePO_4$ is known to have a poor electronic conductivity and it has been reported that smaller grain/particle size has a beneficial effect on high-rate capacity [3,6,13–15]. Consequently, understanding the kinetic behavior of $LiFePO_4$ synthesis is certainly fundamental to the optimization of the synthesis condition.

In the conventional, *isothermal* methodology for studying a solid-state reaction, reaction conversion was measured as a function of time at constant temperature. Significant error is often introduced when reaction already proceeds to an appreciable extent before the reacting powder is heated to and stabilized at the selected temperature. This type of error is particularly serious for reaction of high activation energy, and it turned out to be the case for the present system as observed in our prelim-

* Corresponding author. Tel.: +886 2 23627158; fax: +886 2 23623040.
E-mail address: nlw001@ntu.edu.tw (N.-L. Wu).

0378-7753/$ – see front matter © 2005 Elsevier B.V. All rights reserved.
doi:10.1016/j.jpowsour.2005.09.005

Table 1
Synthesis processes for $LiFePO_4$

Starting materials			Calcination conditions	Reference
Li source	P source	Fe source		
Li_2CO_3	$(NH_4)_2HPO_4$	$Fe(CH_3CO_2)_2$	800 °C, 24 h in Ar	[1]
Li_3PO_4	$Fe_3(PO_4)_2{\cdot}8H_2O$		700 °C, 7 h in Ar	[2]
Li_2CO_3	$(NH_4)_2HPO_4$	$FeC_2O_4{\cdot}2H_2O$	800 °C, 36 h in N_2	[3]
$LiNO_3$	$(NH_4)_2HPO_4$	$Fe_3(NO_3)_3{\cdot}9H_2O$	750 °C, 12 h in Ar	[4]
LiCl	H_3PO_4	$FeCl_2{\cdot}4H_2O$	700 °C, 12 h in N_2	[5]
Li_2CO_3	$NH_4H_2PO_4$	$Fe(CH_3CO_2)_2$	550 °C, 24 h in N_2	[6]
Li_2CO_3	$Fe[(C_6H_5PO_3)(H_2O)]$		>600 °C, >16 h in N_2	[7]
Li_2CO_3	$NH_4H_2PO_4$	$FeC_2O_4{\cdot}2H_2O$	600–800 °C in Ar	[8]
$Li(CH_3COO)$	H_3PO_4	$Fe_3(NO_3)_3{\cdot}9H_2O$	(Sol–gel) 500 °C 10 h in N_2, 600 °C 10 h in N_2	[9]
LiH_2PO_4		Fe_2O_3	750 °C, 8 h in Ar	[10]
Li_3PO_4	$FePO_4$, Fe		600 °C, 30 min in Ar	[11]
Li_3PO_4	$Fe_3(PO_4)_2{\cdot}5H_2O$		550 °C, 15 min in N_2	[12]

inary study. To overcome this problem, as reported here, we have adopted a *non-isothermal* approach to study the kinetics of $LiFePO_4$ formation via a solid-state reaction, where reactant powder was heated at constant rates and the composition of the powder was continuously monitored by synchrotron X-ray diffraction (XRD) as a function of temperature. Reaction conversion data were subsequently determined from the XRD patterns. Accordingly, the kinetic equations were analyzed in terms of their derivatives with respect to temperature for determining kinetic parameters, and finally a consistent kinetic equation that is capable of predicting conversion under isothermal process was derived. In brief, it was determined that the formation of the olivine compound via solid-state reaction has a rather fast intrinsic kinetics, and a conversion of 95% can be achieved, for instance, at 600 °C in 1 h. However, the reaction could be seriously hindered by slow gas-phase diffusion rates of the gaseous reducing reactant and by-products species involved in the reaction.

2. Experimental

In-situ synchrotron XRD was conducted by using beam-line 01-C2 in National Synchrotron Radiation Research Center, Taiwan, ROC, and an X-ray source of 0.061993 nm in wavelength was employed. Reactant mixture containing $Li(CH_3COO)$ and $FePO_4$ with an element stoichiometry of Li:Fe:P = 1:1:1 was filled in a quartz capillary tube (Charles Super Company, 0.7 mm in diameter), and a gas mixture of 1% H_2 in N_2 was allowed to constantly flow through the powder bed. A high-temperature wind blower was employed to heat the powder at selected constant heating rates. A thermocouple was placed in direct contact with the capillary tube at the position where the powder bed was located in order to monitor and control the reaction temperature. XRD patterns were acquired along the course of heating.

Two methods have been adopted to synthesize $LiFePO_4$ powder in larger batches. In the first method, which will hereafter be referred to as the *packed-bed* method, reactant mixture of 8.3 g was loaded inside a vertical quartz tube, and a gas flow containing 1% H_2 in N_2 was passed through the powder bed. This method has a powder-bed geometry and a flow pattern similar to those for synchrotron XRD studies. Alternatively, in the *pellet* method, the reactant mixture was compacted under a pressure of 0.17 ton cm^{-2} to produce reactant pellets with a diameter of 1 cm and a thickness of about 0.8 cm, and the pellets were subsequently heat-treated in a horizontal quartz tube with a flowing gas of the same composition.

For electrochemical characterization, the $LiFePO_4$ electrode was made of 86 wt.% $LiFePO_4$ powder, 6 wt.% carbon black and 8 wt.% organic binder on an Al current collector. After being dried at 150 °C in a vacuum oven for 6 h, the electrode sheets were punched into 1.2 cm-diameter disks for assembly, and every disk typically contains ~6 mg of the olivine with 100 μm in thickness. The coin cell consists of a $LiFePO_4$ disk electrode, a Li foil disk as the counter electrode and electrolyte of 1 M $LiPF_6$ in a 1:2 v/v mixture of ethylene carbonate (EC) and ethyl methyl carbonate (EMC). All the cells were assembled in a dry room where the dew point was maintained at between −40 and −45 °C. The cells were cycled between 2.5 and 4.3 V at 0.05 C rate by using a charge-discharge tester (Bitrode, model: MCN6410) at room temperature.

3. Results and discussion

3.1. Kinetic analysis

Fig. 1 shows some of the XRD patterns that were acquired along the course of heating (reaction) at the heating rate of 0.60 °C min^{-1}. In this run, $LiFePO_4$ started to appear at 420 °C along with other intermediate compounds. Up to 505 °C, both $LiFePO_4$ and the intermediate compounds were presented in appreciate amounts. These impurities could be Li_3PO_4 [8]. Above 505 °C, the intensities of the reflections of $LiFePO_4$ continue to increase, while those of the intermediate compounds first increase and then decrease, with increasing temperature. At 605 °C, the powder became single-phased $LiFePO_4$, and pattern remains unchanged till 700 °C (not shown). The peaks of $LiFePO_4$ were found to shift slightly toward smaller 2θ angles with increasing temperature due to gradual increasing in lattice spaces.

To convert the XRD patterns into kinetic data, the (0 1 1) peak ($2\theta = 8.312$ in Fig. 1) of the olivine compound was used

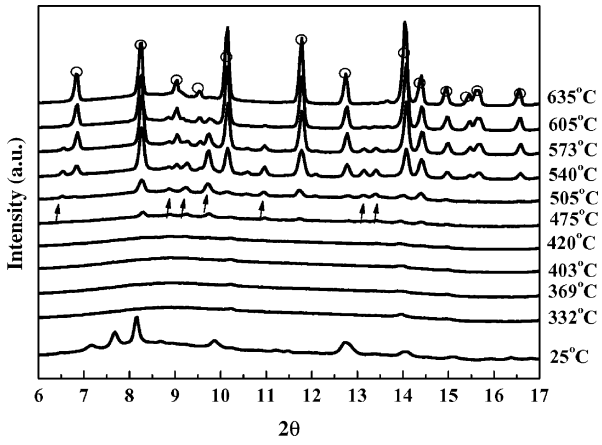

Fig. 1. In situ synchrotron XRD patterns acquired during synthesis of $LiFePO_4$ at the heating rate of 0.60 °C min^{-1}. The arrows indicate the impurity phase Li_3PO_4, and the hollow circles indicate the peaks of $LiFePO_4$.

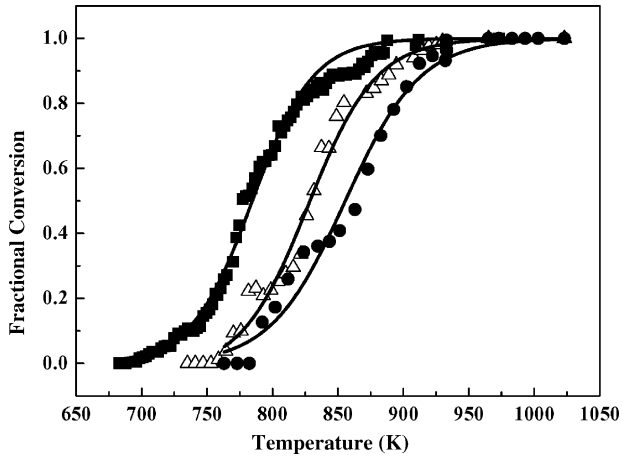

Fig. 2. The fractional conversions for three adopted heating rates, ■: 0.60 °C min^{-1}; △: 2.87 °C min^{-1}; and ●: 4.93 °C min^{-1}. The three curves are fitted based on Boltzmann function.

for calculation. From XRD theory, it is clear that the integrated intensity, i.e. the area under the peak, of a reflection is proportional to the amount of the associated compound presented in the power. For each run with a selected heating rate, the state of "complete reaction", i.e. the state where fraction conversion to $LiFePO_4$, F, is equal to 1.0, is set at the temperature T^* where the powder becomes single-phased $LiFePO_4$ and the intensity of the (0 1 1) peak becomes invariant with further increase in temperature. Accordingly, the fractional conversion F at any temperature T can be calculated from the intensity ratio:

$$F(T) = \frac{I(T)}{I(T^*)}, \quad (1)$$

where $I(T)$ is the integrated intensity of the (0 1 1) reflection acquired at temperature T, while $I(T^*)$ is that at T^*. Fig. 2 shows the conversion data thus calculated for the three adopted heating rates. It was found that the reaction-onset temperature was found to shift to higher temperatures with increasing heating rate, while the temperature range from reaction-onset to completion was narrowed. As described below, the analysis in deriving the governing rate equation in the present study deals mainly with the derivative of the conversion with respect to temperature. When the derivatives are calculated directly from the raw conversion data shown in Fig. 2, they are widely scattered and it becomes impossible to extract meaningful information from them. To avoid this, the conversion data (Fig. 2) were first fitted by Boltzmann equation, which has a form of:

$$F(T) = 1 - \frac{1}{1 + \exp[(T - T_0)/\delta]}$$

where T_0 is the T value at $F = 50\%$, and δ is a fitting parameter. The fitted $F(T)$ lines (solid lines in Fig. 2) were then used to generate the "smoothed" derivative data for further analysis.

As summarized in Table 2, several kinetic rate equations that are commonly used for describing solid-state reaction have been evaluated. They include those summarized by Blazek [16] and by Gadalla and Hegg [17] for the reaction limited by different mechanisms, including nuclei growth, diffusion, and interfacial reaction, respectively. In addition, equations of simple power law and equation of exponential law were also tested. In general, all

Table 2
Summary of the kinetic equations

Rate-limiting mechanism	Kinetic equation $G(F) = k_0 \exp(-E/RT)t$	
	$G(F)$	dG/dF
Nuclei growth		
Two-dimensional	$[-\ln(1-F)]^{1/2}$	$[2(1-F)]^{-1}[-\ln(1-F)]^{-0.5}$
Three-dimensional	$[-\ln(1-F)]^{1/3}$	$[3(1-F)]^{-1}[-\ln(1-F)]^{-2/3}$
Diffusion		
One-dimensional	F^2	$2F$
Two-dimensional	$(1-F)\ln(1-F)+F$	$-\ln(1-F)$
Three-dimensional	$1–3(1-F)^{2/3}+2(1-F)$	$2[(1-F)^{-1/3}-1]$
Interfacial reaction		
Two-dimensional	$1-(1-F)^{1/2}$	$(1/2)(1-F)^{-0.5}$
Three-dimensional	$1-(1-F)^{1/3}$	$(1/3)(1-F)^{2/3}$
Exponential law	$\ln F$	$1/F$
Power-law (nth order)	$(1/n)[1/(1-F)^n]$	$1/(1-F)^{n+1}$

these equations have the form of:

$$G(F) = k_0 \exp\left(\frac{-E}{RT}\right) t, \tag{2}$$

where G is a function expressed in terms of the fractional conversion, F, k_0, the rate constant, which is independent of temperature, T, and E, the activation energy. Eq. (2) can be employed for analyzing the kinetic data under either isothermal or non-isothermal process. For the latter, under a constant heating rate β, the derivative of Eq. (2) with respect to t gives:

$$\beta \frac{dG}{dF}\frac{dF}{dT} = k_0 \exp\left(\frac{-E}{RT}\right)\left\{1 + \left[\frac{E(T-T_0)}{\beta RT^2}\right]\right\} \tag{3a}$$

or

$$\ln\left[\beta \frac{dG}{dF}\frac{dF}{dT}\right] = \ln k_0 - \frac{E}{RT} \ln\left\{1 + \left[\frac{E(T-T_0)}{\beta RT^2}\right]\right\}, \tag{3b}$$

where β is the constant heating rate (dT/dt); dG/dF, the derivative of $G(F)$ with respect to F (Table 2); dF/dT, the derivative of F with respect to T; and T_0, the onset temperature of the reaction at the selected heating rate. For brevity, we will hereafter define a quantity Y to be equal to the left-hand-side of Eq. (3b), i.e.,

$$Y \equiv \ln\left[\beta \frac{dG}{dF}\frac{dF}{dT}\right]. \tag{4}$$

As the third-term of the right-hand-side of Eq. (3b) is expected to be much smaller than the second-term, because of the logarithm, Eq. (3b) has often been simplified [17,18] into:

$$Y \sim (\ln k_0) - \frac{E}{RT}. \tag{5}$$

Eqs. (3a)–(5) suggest two criteria for selecting a consistent rate equation based on the plot of $Y(\equiv \ln[\beta(dG/dF)(dF/dT)])$ versus $1/T$. First, the kinetic equation should give a negative slope throughout the entire non-isothermal reaction process. Secondly, for data collected at different heating rates (β's), they should fall on the same plot.

Fig. 3a–c show the Y–$(1/T)$ plots for all the rate equations listed in Table 2 using the "smoothed" derivative data set for $\beta = 0.60\,^{\circ}\mathrm{C\,min^{-1}}$. It was found that only the equation of power law gives a negative slope throughout the entire reaction temperature range for all three heating rates adopted. Furthermore, for the power-law equations, the criterion that requires the minimum scattering among data of different heating rates gives an optimum reaction order of 0.7 (Fig. 4). In this case, the experimental Y–$(1/T)$ plot is almost linear, and the pre-exponential constant k_0 and activation energy E were determined to be $2.23 \times 10^{11}\ \mathrm{min^{-1}}$ and 47.9 kcal, respectively. This gives a complete rate equation to be:

$$\frac{1}{0.7}\frac{F^{0.7}}{(1-F)^{0.7}} = 2.23 \times 10^{11} \exp\left(\frac{-24,100}{T}\right) t. \tag{6}$$

Once the rate equation and its kinetic parameters were determined, by numerically integrating Eq. (3a), one can simulate the F–T plots for different heating rates. Fig. 5 compares the experimental and simulated conversion data, indicating that the proposed rate equation, Eq. (6), gives reasonably good fit to the raw conversion data. The fact that the conversion data are best modeled by power-law rate equation with a non-integral reaction order suggest complex reaction pathways involved in forming the olivine compound via the solid-state reaction route. As a result, the rate equation can only be considered empirical. As shown below, it does serve as a good guidance for scaling up.

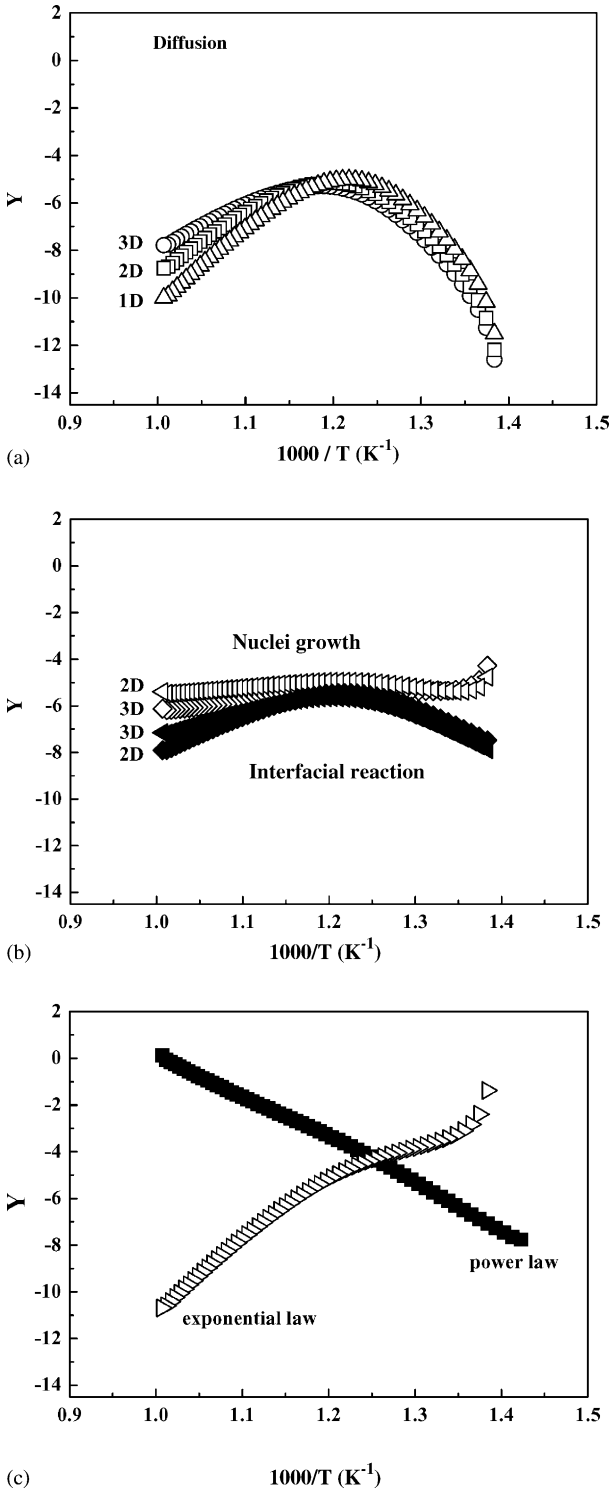

Fig. 3. Y, defined by Eq. (4), plotted against $1/T$ for kinetic equations of: (a) diffusion-limitation; (b) nuclei growth-limitation and interfacial reaction-limiation; (c) power-law and exponential-law.

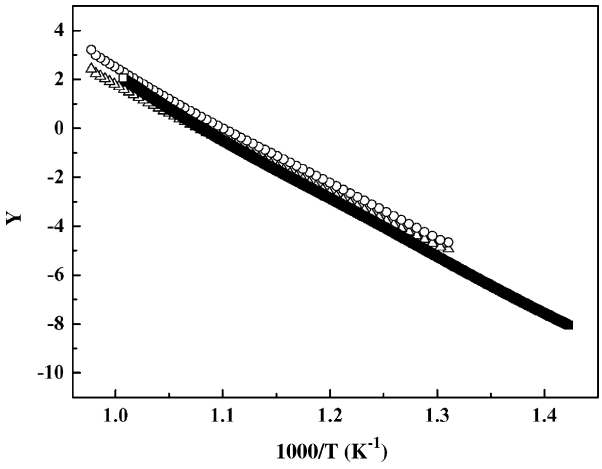

Fig. 4. *Y*, defined by Eq. (4), plotted against $1/T$ at heating rates of: (△) 4.93 °C min^{-1}; (◯) 2.87 °C min^{-1}; (□) 0.60 °C min^{-1}, based on the power-law rate-equation with a reaction order of 0.7.

Once the rate equation is determined, fractional conversion as a function of calcination time during an *isothermal* calcination process at any selected temperature can then be predicted from Eq. (6). Fig. 6 shows the predicted *F–t* plots for some temperatures between 550 and 700 °C. The predicted conversion data indicate that the formation of the olivine compound is a relatively low-temperature, fast reaction: a conversion of 95% can be achieved at 550 °C in less than 5 h, or at 600 °C in 1 h. Although this conclusion was drawn on the basis of a particular set of reactant species used in the present study, it may also be true for other starting reactant reagents. Indeed, the predicted data validate the low-temperature limits, 550–600 °C, that have been adopted in the literature (Table 1), in spite of variations in their starting reactant reagents. The predicted data may also suggest that many of the previous studies might have "over-cooked" their powders. The only exception is Ref. [12], which has a thermal budget (15 min at 550 °C) that is significantly less than what would be expected from Eq. (6). In this particular case, the reactant mixture has been processed by high-energy milling, and

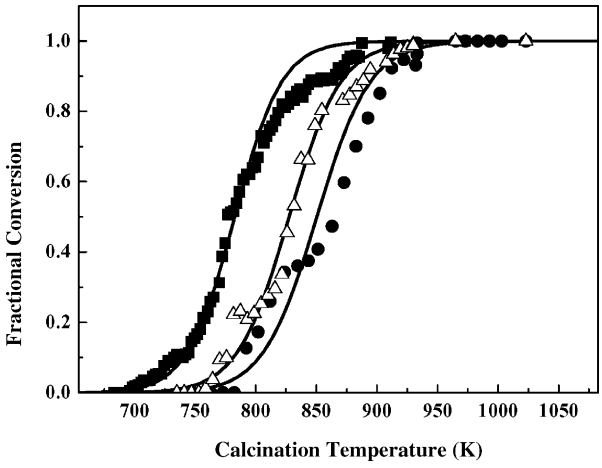

Fig. 5. The fractional conversions for three adopted heating rates (■: 0.60 °C min^{-1}; △: 2.87 °C min^{-1}; and ●: 4.93 °C min^{-1}) and the simulated conversion data (the lines).

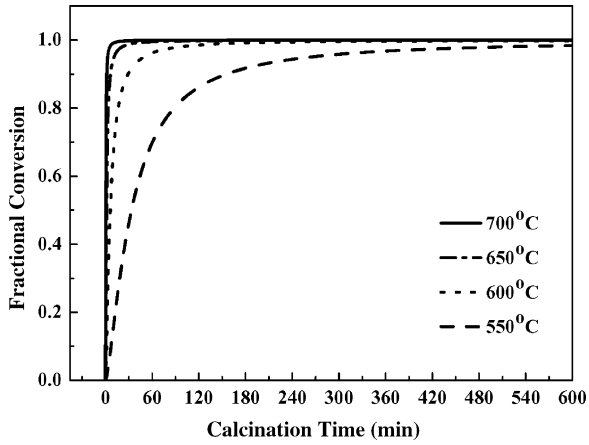

Fig. 6. The predicted fractional conversion vs. calcination time, *t*, for selected temperatures between 550 and 700 °C.

that might have helped to reduce the calcination time during the subsequent thermal treatment at 550 °C.

3.2. Gas-phase diffusion-limitation

The formation reaction of $LiFePO_4$ in the current system may be written as:

$$Li(CH_3COO)_{(s)} + FePO_{4(s)} + 1/2H_{2(g)} \leftrightarrow LiFePO_{4(s)} + CO_{2(g)} + CH_{4(g)}.$$

Formation of CO along with H_2O as gaseous by-products is also likely. Thus, the reaction involves processes of diffusion-in of H_2 and diffusion-out of the listed gaseous products. As these transport processes take place in series with the solid-state reaction process, either one could become rate-limiting, and the overall rate of formation of the olivine compound would be reduced to be lower than that predicted by Eq. (6). In order to understand the effect of the diffusion processes on the rate of $LiFePO_4$ formation, two sets of experimental protocols, namely the packed-bed and pellet methods as described in Section 2, have been adopted. The major difference between these two methods resides in the way the gas flows relative to the reactant mixture. In the packed-bed method, the gas flows *through* the reactant powder bed, and the gaseous reactant/product species would be transported in/out by convective flow. On the other hand, in the pellet method, the gas passes *over* the surfaces of the pellets, and the gaseous reactant/product species have to be transported into/out of the powder bed by diffusion.

It was found that the powders prepared by the packed-bed method always exhibited higher conversions than those by the pellet method after calcination at the same temperature. Fig. 7 compares the XRD patterns of the powders calcined at 700 °C for 0.5 h. The powder synthesized by the packed-bed is single-phased $LiFePO_4$, consistent with that predicted by Eq. (6). In contrast, the powder prepared by the pellet method has a conversion of less than 60%. It is clear that the gas-phase diffusion processes of the reactant/product species have become the rate-limiting in the pellet method. When the rate of formation is limited by gas-phase diffusion, the required calcination temper-

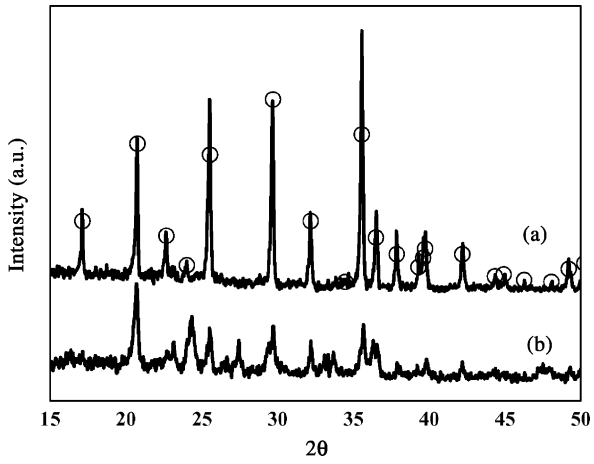

Fig. 7. The XRD patterns of the powders calcined at 700 °C for 0.5 h synthesized by: (a) the packed-bed method; (b) the pellet method. The hollow circles indicate the peaks of $LiFePO_4$.

ature and time for complete conversion will be very sensitive to the batch size and packing density of the powder bed during synthesis. It is presumed that this is one of the reasons that cause wide variations in calcination conditions reported in the literature for $LiFePO_4$ synthesis.

3.3. Electrochemical characterization

A $LiFePO_4$ powder with a batch size of 8 g has been synthesized by using the packed-bed method for electrochemical cycling test. Reactant powders containing additionally of 7 wt.% of carbon black, was calcined at 600 °C for 2 h. Powder XRD analysis of the powder showed single-phase $LiFePO_4$. The average crystallite size calculated by Scherrer equation based on the (0 1 1) reflection is 35 nm. As shown in Fig. 8, the electrode exhibits a redox plateau potential of ~3.5 V, typical of $LiFePO_4$, and the capacities reach ~140 mAh g^{-1}. In spite of the very short calcination time employed, these capacities are comparable with those reported in the literature [19].

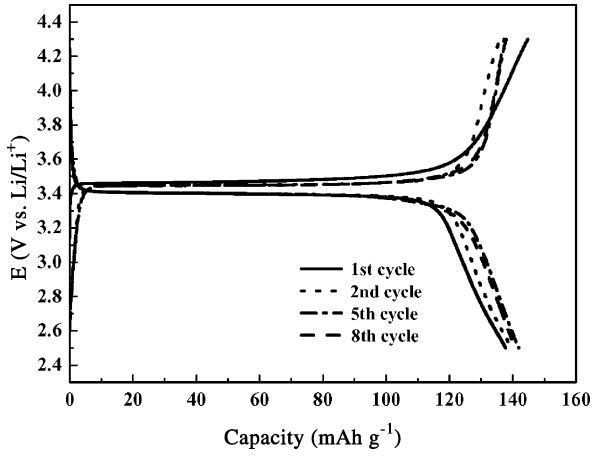

Fig. 8. The charge–discharge curves of the $LiFePO_4$ powder prepared by the packed-bed method.

In addition to calcination to convert the starting reactants to the olivine compound, additional thermal annealing for enhancing its crystallinity could be beneficial to its electrochemical charge/discharge performance. These two thermal processes are usually not clearly distinguished in previous studies. The optimum annealing process for this study has yet to be sought, preferably independently from the calcination process.

4. Conclusions

$LiFePO_4$ was synthesized from mixture of $Li(CH_3COO)$ and $FePO_4$ in a reducing atmosphere, and the kinetics of this reaction was analyzed by using in-situ synchrotron X-ray diffraction measurement and a non-isothermal methodology. The analysis gives a quantitative rate-equation, which indicates that the formation of $LiFePO_4$ is a fast reaction even at temperatures between 550 and 600 °C. Comparative studies using different gas flow pattern, nevertheless, indicate that the reaction rate could be significantly reduced if gas-phase diffusion processes of reactant/product species become rate-limiting, and that the gas-flow pattern relative to the powder bed during synthesis thus has a decisive effect on the reaction rate. Nanocrystalline $LiFePO_4$ powder having an average crystal size of 35 nm has been demonstrated by calcination using flow-through configuration at 600 °C for 2 h, and the powder exhibits a capacity of ~140 mAh g^{-1}.

Acknowledgement

This work was supported by the Materials Research Laboratories, Industrial Technology Research Institute, Hsinchu, Taiwan.

References

[1] A.K. Padhi, K.S. Nanjundaswamy, J.B. Goodenough, J. Electrochem. Soc. 144 (4) (1997) 1188–1194.
[2] M. Herstedt, M. Stjerndahl, A. Nytén, T. Gustafsson, H. Rensmo, H. Siegbahn, N. Ravet, M. Armand, J.O. Thomas, K. Edström, Electrochem. Solid-State Lett. 6 (9) (2003) A202–A206.
[3] A.S. Andersson, B. Kalska, L. Häggström, J.O. Thomas, Solid State Ionics 130 (2000) 41–52.
[4] S.-T. Myung, S. Komaba, N. Hirosaki, H. Yashiro, N. Kumagai, Electrochim. Acta 49 (2004) 4213–4222.
[5] H. Huang, S.-C. Yin, L.F. Nazar, Electrochem. Solid-State Lett. 4 (10) (2001) A170–A172.
[6] A. Yamada, S.C. Chung, K. Hinokuma, J. Electrochem. Soc. 148 (3) (2001) A224–A229.
[7] E.M. Bauer, C. Bellitto, M. Pasquali, P.P. Prosini, G. Righini, Electrochem. Solid-State Lett. 7 (4) (2004) A85–A87.
[8] S.-Y. Chung, J.T. Bloking, Y.-M. Chiang, Nature Mater. 1 (2002) 123–128.
[9] Y. Hu, M.M. Doeff, R. Kostecki, R. Fiñones, J. Electrochem. Soc. 151 (8) (2004) A1279–A1285.
[10] J. Barker, M.Y. Saidi, J.L. Swoyer, Electrochem. Solid-State Lett. 6 (3) (2003) A53–A55.
[11] X.-Z. Liao, Z.-F. Ma, L. Wang, X.-M. Zhang, Y. Jiang, Y.-S. He, Electrochem. Solid-State Lett. 7 (12) (2004) A522–A525.

[12] S. Franger, F. Le Cras, C. Bourbon, H. Rouault, Solid-State Lett. 5 (10) (2002) A231–A233.
[13] M. Takahashi, S. Tobishima, K. Takei, Y. Sakurai, J. Power Sources 97–98 (2001) 508–511.
[14] A.S. Andersson, J.O. Thomas, B. Kalska, L. Häggström, Electrochem. Solid-State Lett. 3 (2000) 66–68.
[15] S. Okada, S. Sawa, M. Egashira, J. Yamaki, M. Tabuchi, H. Kageyama, T. Konishi, A. Yoshino, J. Power Sources 97–98 (2001) 430–432.
[16] A. Blazek, Thermal Analysis, Van Nostrand Reinhold, London, 1973, p. 64.
[17] A. Gadalla, D.T. Hegg, Thermochim. Acta 145 (1989) 149–163.
[18] N.L. Wu, T.C. Wei, S.Y. Hou, S.Y. Wong, J. Mater. Res. 5 (1990) 2056–2065.
[19] K. Striebel, J. Shim, V. Srinivasan, J. Newman, J. Electrochem. Soc. 152 (4) (2005) A664–A670.